VIII International Conference on Fracture Mechanics of Concrete and Concrete Structures
FraMCoS-8
J.G.M. Van Mier, G. Ruiz, C. Andrade, R.C. Yu and X.X. Zhang (Eds)

FRACTURE BEHAVIOUR OF CONCRETE AT HIGH STRAIN RATE

EZIO CADONI*

* University of Applied Sciences of Southern Switzerland, DynaMat Laboratory
Campus SUPSI – Trevano, 6952 Canobbio, Switzerland
e-mail: ezio.cadoni@supsi.ch, www.dynamat.supsi.ch

Key words: High strain rate, Impact, Hopkinson bar, Dynamic tensile strength.

Abstract: The design of concrete structures subjected to impact loads needs a significant level of knowledge of the constituent materials behaviour at higher strain-rates. In this paper are analysed the influence of the strain rate on the fracture behaviour considering the tensile strength and fracture energy. A large number of direct tensile tests on plain concrete specimens performed at high strain-rates by means of a modified Hopkinson bar are reviewed. These results at high-strain-rate tests represent different concretes, with different maximum aggregate size, size and curing histories. The experiments had shown a significant increases of the tensile strength, failure strain and fracture energy as the strain-rates increase. Finally, results obtained using a special set-up of modified Hopkinson bar able to follow the crack propagation at high strain rate are presented.

1 INTRODUCTION

The impulsive loads are rare events that may occur in the lifetime of the concrete structures, such as impacts and blasts, which induce different high strain-rates in the materials. Typical such impulsive examples are: collision of vehicles or vessels with bridge piers or superstructures, explosions near or inside structures, impact of projectiles, blast caused by near or far explosions, etc. During such severe applied loads, high strain-rates are imposed on the structures. The range of strain rates for concrete, caused by such accidents, may be very large; typically from ~10^{-1} s^{-1} for severe earthquakes to ~ 10^{2} s^{-1} for very strong explosions. As results, it is necessary that the rate effects in the materials on structural responses should be considered in order to predict structural response realistically.

When a structure is stressed by an impulsive load, the energy does not act immediately on all parts of the structure. In fact, the deformation and stresses caused by the impulsive load propagate through the structure in the form of disturbances like stress and strain waves. This is the most evident difference between the so called quasi-static and the impact load. As a results, the behaviour of the structure differs a lot when it is loaded dynamically instead of statically. In fact, for example in the case of concrete, under low strain rate loading the fracture process starts from existing micro-cracks and macro-cracks and has the time to choose and develop along the path of least energy requirements, i.e., around aggregate particles and through the weakest zones of the matrix. Due to low overall stress level and relaxation of material, the extension of micro-cracks in other areas of higher strength is rather limited. Under impact tensile loading conditions much energy is introduced into the structure in a short time, and cracks as concentration points are forced to develop also along a shorter path of higher resistance - through stronger matrix zones and some aggregate particles. The very rapidly increasing overall tensile stress causes extensive micro-cracking in other areas, since relaxation cannot occur in the extremely short time of fracture.

In the design process the material characteristics and the consequent structural behaviour should be known in a large range of strain rates, in particular the assessment tools used (computer code for example) should be validated for the same strain rate range.

Among the mechanical parameters that are essential to know are: the tensile strength, the ultimate strain, the stress-strain diagram, the fracture characteristics of the material, etc.

Up to now in structural analysis the tensile strength has been neglected, but, indirectly the structural response relies on it because tensile strength greatly influences the cracking behaviour, the bond properties of reinforcing steel and the behaviour under shear force. In particular, when the structures are impacted, they are first subjected to a compressive stress wave which can be very often reflected in the structural elements as a tensile stress wave which is then the main cause of failure of concrete.

In general, the stress waves propagating through the structures deform the structural materials at high strain rate giving rise to cracking process changes different from those taking place at quasi-static strain-rate; such changes might cause a change of the stress-strain curves of the material at high strain-rate with respect to that at quasi-static strain rate.

Therefore dynamic material testing method assuring results of high precision must be designed in such a way that the well proofed elastic stress wave propagation theory can be applied to the analysis of the experimental measurements.

The most satisfactory testing method implementing the elastic stress wave propagation theory so far developed for accurate measurements of the dynamic mechanical properties of materials is the Hopkinson bar technique. It allows the generation of a loading pulse well controlled in rise time, amplitude and duration, giving rise to the propagation of an uniaxial elastic plane stress wave.

In the next paragraphs are described the dynamic direct tension test results and the experimental results adopted.

2 EXPERIMENTAL TECHNIQUES

It is well known that tension test is probably one of the most difficult test on materials in statics and in dynamics. In the case of concrete the measurement of the tensile strength can be done using three methods as direct tension test, bending test and splitting tensile test.

From the theoretical point of view the true tensile test have to be obtained through the direct tension and the material model must be able to describe the real behaviour of the material in the structures. Only after these steps is possible to compare the results obtained by means of other techniques. In fact bending and splitting test results are different from direct tension one. In literature is possible to find many results that are not comparable and often they are contradictory because of the high sensitivity to the shape and size of the specimens used as well as to the testing techniques adopted.

In dynamics the tensile strength has been measured using basically the Hopkinson-Kolsky bar and its modification. The traditional Split Hopkinson Pressure Bar (SHPB) were used to study the indirect tensile strength by splitting test (Figure 1a).

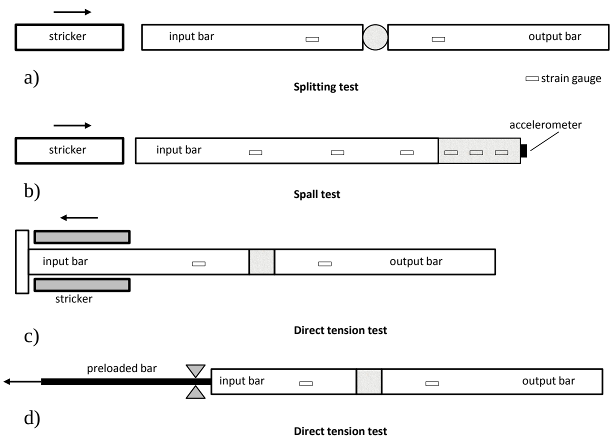

Figure 1: Experimental set-ups for tension test

Other authors used part of SHPB (removing the output bar and using a longer specimen) to investigate the tensile behavior of concrete under high loading rates by spalling test (Figure 1b).

The direct tensile strength was measured by the Hopkinson-Kolsky bar essentially in two configurations: i) using a setup in which the projectile hit the flange of the one bar (Figure 1c); ii) using a pretension bar connected to the input bar to produce the loading pulse (Figure 1d).

Hereafter are described some experimental techniques used to measure the tensile strength of concrete.

2.1 The JRC-Modified Hopkinson Bar

The JRC-Modified Hopkinson Bar (JRC-MHB) shown in Figure 2, is presently placed in the laboratory of the Joint Research Centre of the European Commission at Ispra (Italy).

Figure 2: The JRC-Modified Hopkinson Bar.

It consists of two half-bars (Figure 1d), the input and output bar respectively, with the specimen introduced in between. The input and output bars are aluminum prismatic elements having a length of 2 m and a square section of 60 mm side. The interior extremes of these bars, over a length of 500 mm, are subdivided by wire electro discharge machining into 25 symmetrical pairs of parallel, smaller bars. Aluminum has been chosen as the bar material because of its transverse modulus, which is not far from that of plain concrete. This fact, together with the fine longitudinal cuts on the ends of the aluminum bars glued to the specimen, minimizes the constraint to transverse deformation of the concrete specimen. In this way, specimens with square cross section of 60×60 mm² have been tested. Connected to the input aluminum bar is a high strength steel pretension bar. The pretension bar substitutes the striker bar of the traditional SHPB and is used to store elastic energy.

The principle of operation of the JRC-MHB can be summarized as follows. The pre-tensioned bar is statically pulled by a hydraulic actuator in one end, while the other is fixed by the blocking device. A predetermined amount of elastic energy is thus stored in the system. By releasing this energy (rupturing the brittle piece in the blocking device), a rectangular tensile wave with small rise-time (30μs) is generated and transmitted along the input bar loading the specimen to failure. This tensile wave fulfils the requirements for being a one-dimensional elastic plane stress wave: (i) the wave-length of this pulse is long compared to the bar transverse dimensions, and (ii) the pulse amplitude does not exceed the yield strength of the input and output bars.

The pulse propagates along the input bar with the velocity C_0 of the elastic wave. When the incident pulse (ε_I) reaches the specimen, part of it (ε_R) is reflected by the specimen, whereas another part (ε_T) passes through the specimen propagating into the output bar. The relative amplitudes of the incident, reflected and transmitted pulses, depend on the mechanical properties of the specimen.

Strain gauges mounted on the input and output bars of the device, at equal distances from the specimen, are used for the measurement of the elastic deformation (as a function of time) created on both bars by the incident/reflected and transmitted pulses, respectively. The signals are captured by a transient recorder designed to provide high precision waveform acquisition and analysis capabilities, generally with a maximum sampling frequency of 1 MHz.

The displacements of the two interfaces between concrete specimen and bars are also measured by means of an optoelectronic device Zimmer (of resolution up to 10μm) that measures the movements of a black and white target.

Using the theory of one-dimensional elastic wave propagation in bars stress, strain rate, and strain of the specimen can be calculated:

$$\sigma(t) = E_0 \frac{A_0}{A} \varepsilon_T(t) \qquad (1)$$

$$\varepsilon(t) = -\frac{2C_0}{L} \int_0^t \varepsilon_R(t)\, dt \qquad (2)$$

$$\dot{\varepsilon}(t) = -\frac{2C_0}{L} \varepsilon_R(t) \qquad (3)$$

where: E_0 is the elastic modulus of the bars; A_0 is their cross-sectional area; A is the specimen cross section area; L is the specimen length; C_0 is the sound velocity of the bar material.

2.2 The DynaMat-MHB

Since 2006 the JRC-MHB has been extensively used in the DynaMat laboratory in Lugano (Switzerland) [1-5]. Here are present two types of MHB with cylindrical bars.

The larger one is shown in Figure 3.

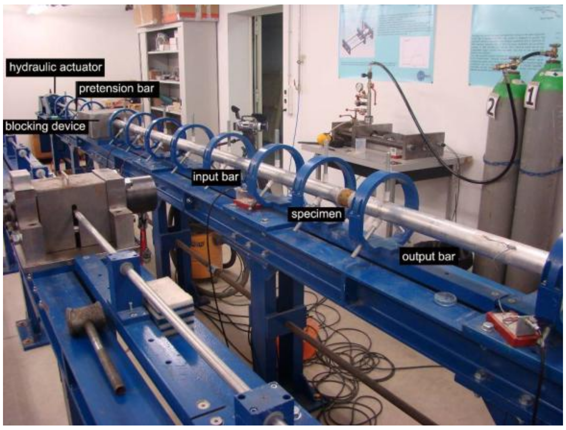

Figure 3: The DynaMat-Modified Hopkinson Bar.

The dimensions of the input and output bars are 60mm in diameter and 3m in length. The pretension bar is a Maraging steel bar of 3m in length and 38mm in diameter in order to have the same acoustical impedance.

The second set-up is composed of two aluminum bars, having 20mm of diameter, 3m and 6m length (input and output bar). The specimen having the same diameter as the input and output bar, is located between them, glued using an high strength epoxy resin. A high strength steel pretension bar, having a length of 6m and a diameter of 12 mm, is directly connected to the input bar and is employed to store elastic energy, which is provided by an hydraulic actuator at one end of the bar and is resisted by a blocking device on the other end. Also in this case the diameter of the pretension bar was chosen in order to have the same acoustical impedance of the aluminum input bar so that undesired wave reflections are avoided.

2.3 The Hopkinson Bar Bundle (HBB)

In 1994 an innovative set-up was developed in order to study the behaviour of standard concrete with real maximum aggregate size [6]. In fact the information on high strain rates tensile concrete behaviour must be gained from experiments performed on specimens of sufficient size to include aggregates of large size (25÷32 mm) in the concrete practically used in the concrete structures. The results obtained on micro-concrete (aggregate size 5÷10 mm) cannot be safely extrapolated to the concrete of real civil engineering structures in which large size aggregates are present. As well known, the Hopkinson bar technique is widely used to determine the mechanical properties of structural materials under high loading rates. Nevertheless the standard Hopkinson bars are sufficient only for dynamic testing of fine-grained materials. Therefore, to load representative concrete specimen with real-size aggregates, a larger Hopkinson bar is needed. For this purpose a special large Hopkinson bar system (Hopkinson Bundle Bar) were developed and installed in the Joint Research Centre at Ispra (Figure 4). The HBB is a special equipment enabling a precise measurement of the stress-strain diagram, including the softening branch, which is important for the correct evaluation of the energy absorption capability of the real concrete used in civil engineering structures. The HBB system consists of two bundles of 25 aluminium bars to which the concrete test specimen is glued using an epoxy resin as shown in Figure 5. The bar bundles were constructed from two aluminium prismatic bars having a length of 2m and a square cross section 200 mm side. The two bars were subdivided by wire-electro-discharging-machine into 25 symmetrical pairs of parallel bars for a length of 1m; the other 1m length remains as a whole. In this way, concrete specimens with square cross section of 200x200 mm² were tested. The strain gauges were glued on 25 bar bundles by means of a micro-blade system. By the strain gauges mounted on each individual bar in the bundles, local measurements of the incident, reflected and transmitted pulses were obtained. These pulses act on each portion of the concrete specimen cross-section facing each symmetrical pair of bars in the bundle. Also the whole portions of the bars were instrumented with strain gauges in order to measure the entire incident, reflected and transmitted pulses acting on the whole cross section of the specimen.

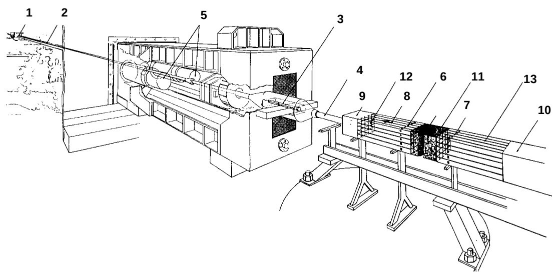

1. hydraulic actuator; 2. high strength steel cables for energy storage (100m); 3. explosive bolt; 4. loading bar; 5. hydraulic dampers; 6. strain gauges to measure incident and reflected pulses; 7. strain gauges to measure transmitted pulses; 8. load direction; 9. instrumented input whole aluminum bar; 10. instrumented output whole aluminum bar; 11. specimen; 12 elementary input bar bundle; 13. elementary output bar bundle.

Figure 4: Hopkinson Bar Bundle experimental set-up

A test with the HBB is performed as follows:

- a hydraulic actuator, of maximum loading capacity of 5 MN, is used to pull 32 cables of high strength steel having a length of 100 m; the pretension stored in these cables is resisted by one grounded explosive bolt in the blocking device (see Figure 4);
- the second operation is the rupture of the explosive bolt which gives rise to a tensile mechanical pulse of 40 ms duration with linear loading rate during the rise time, propagating along the Hopkinson bar bundle and bringing to fracture the plain concrete specimen. Different strain-rates are obtained varying the load on pretension system.

Thanks to the local measurements the history of the single portion of the concrete specimen were studied. From these information is possible to follow how the specimen locally behaves and the crack propagation at high strain rate.

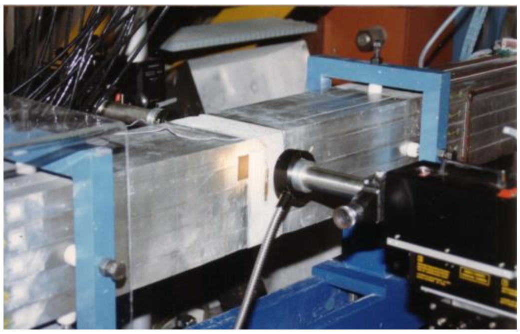

Figure 5: Hopkinson Bar Bundle experimental set-up

3 FRACTURE PROCESS AT HIGH STRAIN RATE

The cracking process of concrete subjected to tensile loading is normally described using a fracture mechanics approach. The behaviour in tension can be represented by different phases. First of all it must be recalled that due to shrinkage of the matrix restrained by the aggregate in the material, micro-damage is present. It is possible to find micro-cracks with the same probability in all volume elements because they are randomly distributed. Whilst the stress increases, these micro-cracks grow and crack localisations take place, forming some macro-cracks. Finally, the macro-cracks propagate leading to failure the specimen.

When the strain-rate is increased from $1s^{-1}$ to $10s^{-1}$ the stress wave propagation effects on the cracking process changes have to be taken into account.

In fact, while in the static case the crack chooses the way with the minimum energy requirement (i.e. matrix-aggregate interfaces), in the dynamic one the wave propagation also induces cracking in the tougher aggregate. Using the information obtained from the bundle bar it is possible to describe the mode and the growth of the fracture through the cross-section of the specimen.

The fracture propagation has been represented by means of diagrams in which the positions of cracks at successive times on the specimen cross-section have been indicated by isochronous curves. In Figures 6-13 the strength distribution (a) and the crack propagation (b) are shown for concrete with 25mm maximum aggregate size, at different curing conditions, at 1 and 10 s^{-1} respectively. The numbers shown in the grid represent the local strength measured by the elementary bars. It can be observed as the average value of the local strength σ_{av} are the same measured in the whole bar σ_0. In figures (b) are indicated the isochronous curves of the positions of the cracks during the fracture process. It can be noted that in the case of impact load there is not an unique crack starting and growing from a single point but there are many macro-cracks starting simultaneously and propagating from many points; in other words the multi-activation of cracks is present.

The multi-activation of cracks leading to fracture is also confirmed by the observation that in the very short time of about 20μs the crack initiation is spread all over the specimen cross-section. The multi-activation of fracture is an effect of the impact loading. Cracks are growing so rapidly and are so well distributed over the specimen cross-section that the pulse accelerates all material particles and there is no time to concentrate the load only on the weakest place; many weak points are simultaneously brought to fracture by the load wave. In the tests carried out at strain-rate of 1s^{-1} is evident that a single crack propagates through the cross section, and the cracking process takes more than 50μs to cover the entire cross section [7-8].

The effect of the relative humidity is also highlighted in the duration of the cracking process. In the dried specimen the duration is about 15μs while in the wet specimen the duration is about 60μs [9].

5.22	5.46	5.27	4.65	4.22
4.92	5.39	4.90	4.41	4.02
4.42	5.46	5.08	4.62	3.84
4.94	5.25	4.66	4.83	3.21
5.00	5.32	4.89	4.62	4.23

a)

σ_{av}= 4.76 MPa; σ_0= 4.78 MPa

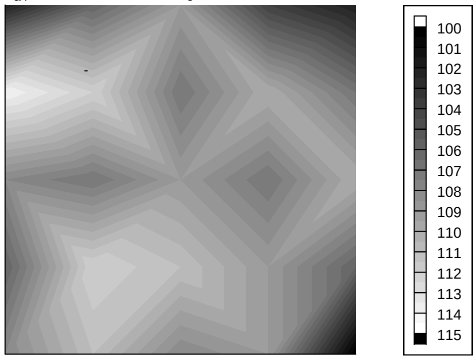

b)

TEST 2173#3 (isochronous in μs)

Figure 6: Specimen dried tested at 10 s^{-1}:
a) Strength distribution; b) crack propagation.

4.79	5.37	5.40	4.91	3.97
4.28	5.17	5.37	4.86	4.44
4.02	4.96	5.08	4.81	4.59
3.88	4.89	4.73	4.85	3.88
4.69	5.17	5.12	4.90	4.53

a)

σ_{av}= 4.75 MPa; σ_0= 4.54 MPa

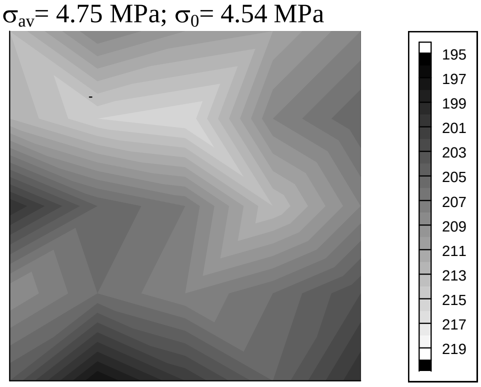

b)

TEST 2173#6 (isochronous in μs)

Figure 7: Specimen dried tested at 1 s^{-1}:
a) Strength distribution; b) crack propagation.

a)

6.81	7.16	7.94	7.66	6.84
6.09	6.60	7.85	7.74	7.32
5.50	6.75	7.26	7.53	7.37
5.67	6.51	6.60	7.24	6.96
4.76	7.26	7.44	7.62	7.43

σ_{av}= 6.98 MPa; σ_0= 6.57 MPa

b)

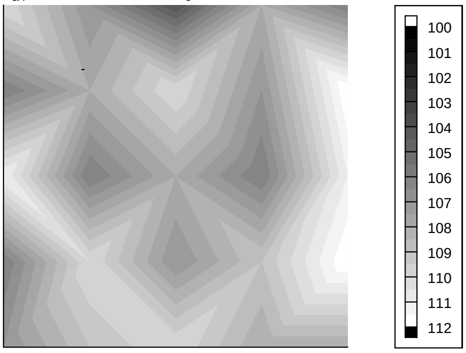

TEST 2170#1 (isochronous in μs)

Figure 8: Specimen at 50% R.H. tested at 10 s^{-1}:
a) Strength distribution; b) crack propagation.

a)

4.95	6.09	6.81	6.58	5.54
4.36	5.77	6.73	6.50	5.78
5.59	5.08	6.11	6.39	5.92
4.09	5.45	5.60	6.52	5.20
4.05	5.86	6.32	6.48	6.18

σ_{av}= 5.76 MPa; σ_0= 4.99 MPa

b)

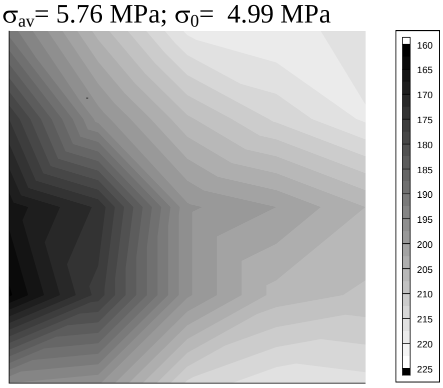

TEST 2170#4 (isochronous in μs)

Figure 9: Specimen at 50% R.H. tested at 1 s^{-1}:
a) Strength distribution; b) crack propagation.

a)

9.97	10.75	10.35	9.36	8.30
8.22	10.25	10.50	9.78	9.17
9.05	9.85	9.46	9.87	9.23
8.04	8.20	8.99	9.40	7.87
4.19	7.33	9.49	9.64	9.80

σ_{av}=9.09 MPa; σ_0= 9.06 MPa

b)

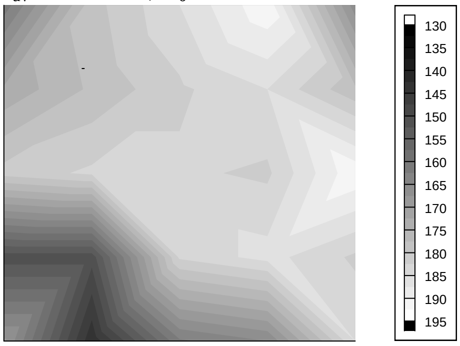

TEST 2174#1 (isochronous in μs)

Figure 10: Specimen wet tested at 10 s^{-1}:
a) Strength distribution; b) crack propagation.

a)

6.13	6.61	6.85	6.68	5.79
5.00	6.11	6.31	6.26	5.86
4.60	5.52	5.44	5.80	5.72
4.19	5.02	5.01	5.34	4.51
4.24	4.61	4.99	5.13	4.95

σ_{av}= 5.47 MPa; σ_0= 5.48 MPa

b)

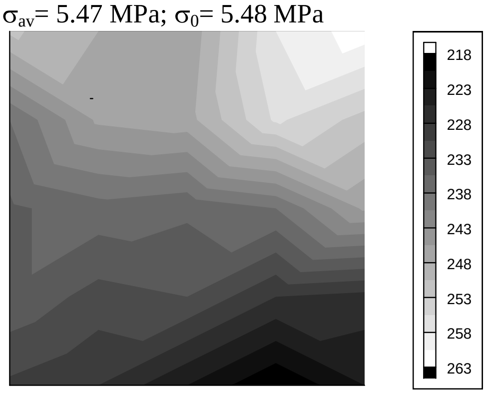

TEST 2174#6 (isochronous in μs)

Figure 11: Specimen wet tested at 1 s^{-1}:
a) Strength distribution; b) crack propagation.

a)

10.53	11.27	11.12	11.50	9.71
8.45	8.95	10.30	11.12	8.60
7.97	8.93	9.95	9.44	9.81
7.45	9.50	9.10	9.38	8.73
9.55	11.12	11.13	10.86	10.08

σ_{av}= 9.79 MPa; σ_0= 8.42 MPa

b)

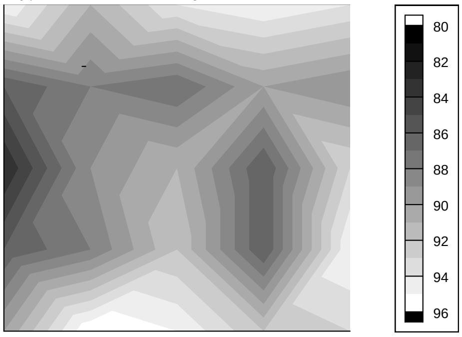

TEST 2194#3 (isochronous in µs)

Figure 12: Specimen tested at 10 s^{-1}:
a) Strength distribution; b) crack propagation.

a)

6.85	7.72	8.29	8.10	6.72
5.90	7.29	7.97	7.82	6.71
5.64	7.15	7.20	7.63	7.02
5.74	6.71	6.66	7.35	5.67
6.09	6.73	7.11	7.27	6.47

σ_{av}= 6.96 MPa; σ_0= 6.57 MPa

b)

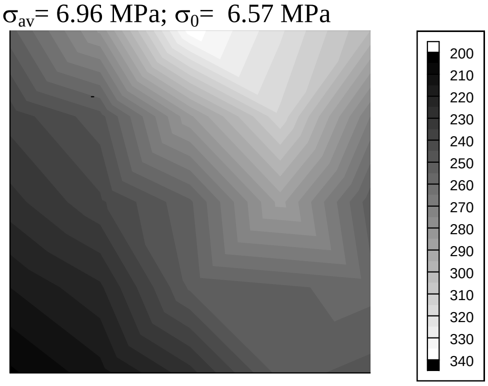

TEST 2194#4 (isochronous in µs)

Figure 13: Specimen tested at 1 s^{-1}:
a) Strength distribution; b) crack propagation.

4 REVIEW OF THE RESULTS

Hereafter the review of the results obtained with the facilities above described useful to the discussion. As known an increase of the concrete mechanical characteristics, such as strength, ultimate strain, elastic modulus and fracture energy, is observed as the strain-rate increases [10]. In Figure 14 the stress versus strain curves in direct tension at different strain rates are depicted.

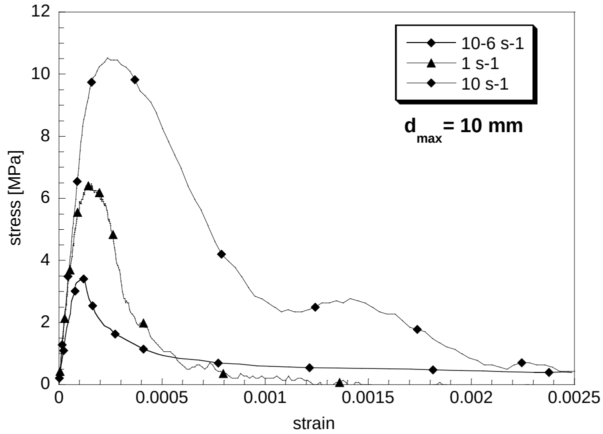

Figure 14: Comparison of the stress vs. strain curves at different strain rates in tension.

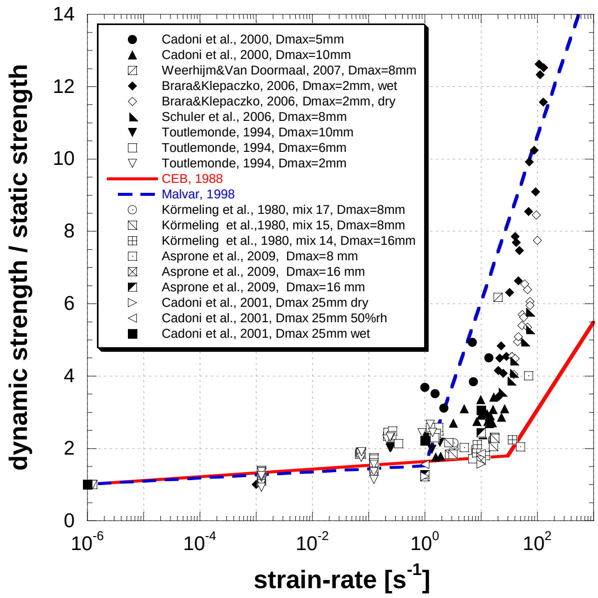

Figure 15: DIF vs. strain-rate in tension.

The description of the rate sensitivity in concrete is normally expressed by the ratio of the dynamic to the static value of a particular mechanical property. Special attention has been addressed to the concrete strength, where this ratio is called the Dynamic Increase Factor

(DIF), and can be useful in numerical code formulations. Such descriptions of the concrete behaviour under impact can be found in [10], while updated models for the increase of strength with strain-rate are presented in [11].

In Figure 15 are shown the DIF versus strain rate of the tension strength and the proposed formulation.

The current constitutive laws for concrete tend to include more information about the material characteristics, for example, the ultimate strain or fracture energy, and this imposes further demands on testing.

4.1 Influence of free water content

The free water in the concrete modifies its behaviour at high strain rate. Normally the problem is studied on micro-concrete in two conditions of relative humidity (wet and dry). It has been found that tensile strength increase with increasing relative humidity. This increment has been explained with the Stefan effect [12] or with the wave propagation consideration [9].

The test results obtained with HBB on concrete with large aggregates size, showed how the loading rate effect is governed by the wave propagation in the material in dynamic case (high strain-rate) while in the quasi-static case the cracking process is governed by the micro-cracking of the material.
The difference in term of strength between dried and wet concrete were explained considering the wave propagation on the pore filled with water or void. In the last case the pore reflects locally the incoming stress wave increasing the stress by multiple reflections obtaining material damage. At the contrary when a stress wave meets a saturated pore greater part of it is transmitted and the residual part is reflected and is not sufficient to cause the stress increase and damage (the crack starts later as shown in Figures 6-7 and 10-11). For that reason wet concrete exhibits less damage and more pronounced rate-dependent effects than dry concrete when subjected to stress waves. In Figure 16 are shown the stress versus time of the three specimens wet, dried and with 50% of relative humidity.

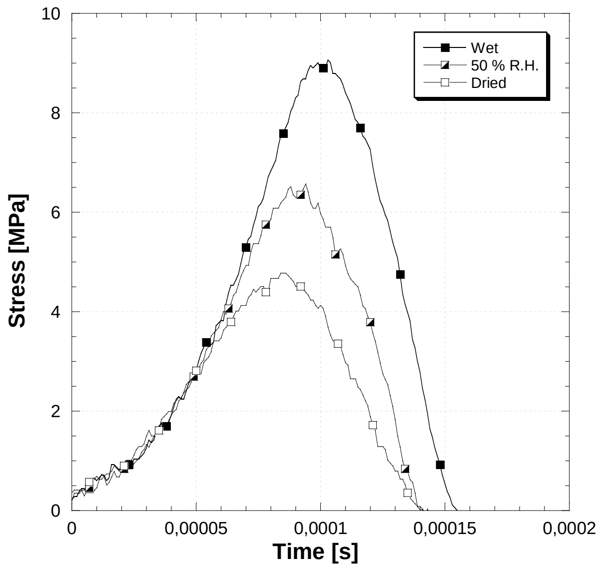

Figure 16: Stress vs. time of three conditions.

The same behaviour was not observed in the case of quasi-static regime, the free water influence does not exist at all. In fact a small decrease in tensile strength was observed for wet concrete specimens due to the action of water pressure occurring in the water filled voids that produce a "wedge effect" decreasing the quasi-static bearing capacity of the material.

4.2 Influence of the aggregate size

Observing the results of previous experimental campaigns [10-11] it can be stated that at high strain rates, the uniaxial tensile strength of concrete decreases with increasing maximum size of aggregate particles. Decreasing the maximum aggregate size the surface area of the aggregate is increased [13]. As results the percentage of voids decreases, positively influencing the bond strength between cement paste and aggregate particles.

Table 1: Results of two types of concrete [14]

Max. aggr. size	Strain-rate [s^{-1}]	Loading rate [GPa/s]	Tensile strength [MPa]	Failure strain [με]	Fracture energy [J/m²]
5mm	*9.4*	*240*	*11.8*	*207*	*377*
	1.6	*169*	*9.2*	*128*	*222*
10 mm	*14.6*	*228*	*10.5*	*236*	*448*
	2.6	*95*	*7.4*	*167*	*183*

4.3 Influence of the specimen size

Experiments were performed on small (60x60mm) and large (200x200mm) specimens on two similar Hopkinson bar set-ups described in previous paragraphs. The mean tensile strength for the two sizes are reported in Table 2.

Table 2: Results of two specimen sizes [13]

Strain rate [s^{-1}]	Tensile Strength (60 mm side) [MPa]	Tensile Strength (200 mm side) [MPa]
10	10.52	8.63
1	7.37	6.68
10^{-6}	3.61	3.57

These results are influenced by strain rate and inertial effects. These two phenomena should be uncoupled by means of numerical simulations. The specimen size influences the mechanical characteristics at high strain rate and these phenomena should be studied more in detail.

5 DISCUSSION

The tensile strength as well as the fracture energy are strain rate sensitive. As shown in Figure 14 the fracture energy increase with increasing strain rate. In Figure 17 the fracture energy in function of the strain rate that several authors have found [14-17].

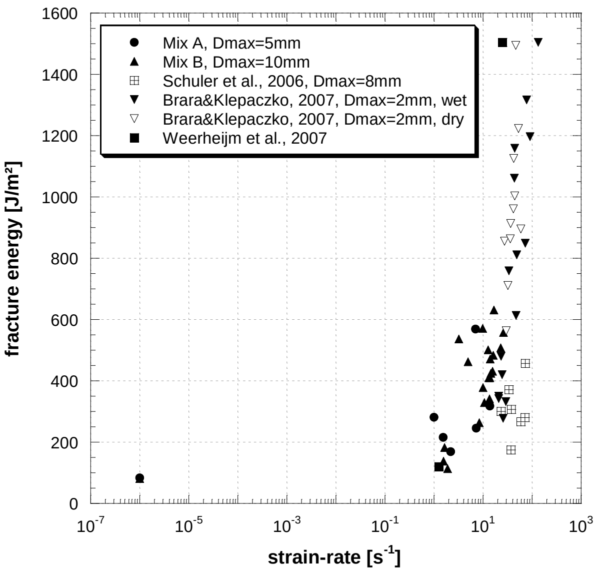

Figure 17: Fracture energy vs. strain rate [14].

These values were obtained using both spalling and direct tension tests. In the case of fracture energy in dynamics many factors have to be controlled and not all experimental techniques permit to follow the cracking process. It has been demonstrated as HBB can be one of the solution to fit these needs.

Regarding the DIF formulation proposed in literature some remarks are necessary. These formulation were obtained by the fitting of a large number of results obtained by many authors with several experimental techniques. They take into account only the compressive strength of the concrete and do not consider other important variables as maximum aggregate size, free water content, specimen size, experimental set-up, etc. The fracture behaviour of concrete has still many aspects open and requires more experimental and numerical studies addressed to the description of the influence of the significant parameters as the cement content, cement type, aggregate type, water/cement ratio, etc.

Finally more efforts should be concentrated on the development of recommendations on the experimental measurement of the dynamic tensile strength. These can be obtained only after a round robin between the worldwide laboratories and supported by the efficient action of numerical simulation, obtaining the comprehension of the relationships between different testing systems and corresponding conversion factors. From this point it will be possible to eliminate the gap between materials and structural tests through the validation of the numerical codes.

REFERENCES

[1] Asprone, D., Cadoni, E., Prota, A. 2009. Experimental analysis on tensile dynamic behavior of existing concrete under high strain rates, *ACI Str J*, **106**:106-113.

[2] Asprone D., Cadoni E., Prota A., and Manfredi G., 2009. Dynamic behavior of a Mediterranean natural stone under tensile loading. *Int J Rock Mech Min Sci*, **46**:514–520.

[3] Cadoni, E., 2010. Dynamic characterization of orthogneiss rock subjected to intermediate and high strain rates in tension. *Rock Mech. and Rock Engg.*, **43**: 667-676.

[4] Cadoni, E., Meda, A., and Plizzari, G., 2009. Tensile behaviour of FRC under high strain-rate. *Mat. and Struct.*, **42:** 1283-1294.

[5] Caverzan, A., Cadoni, E. and di Prisco, M. 2012. Tensile behaviour of high performance fibre-reinforced cementitious composites at high strain rates. *Int. J. of Impact Engg*., **45**:28-38.

[6] Albertini, C., Cadoni, E. and Labibes, K. 1999. Study of the mechanical properties of plain concrete under dynamic loading. *Exp. Mech.* **39**:137-141.

[7] Albertini, C., Cadoni, E., Labibes, K., 1997. Impact fracture process and mechanical properties of plain concrete by means of an Hopkinson bar bundle, J. de Phys. IV, Vol.III, N.7, 915-920.

[8] Cadoni, E., Labibes, K., Berra, M., Giangrasso, M., Albertini, C., 2000. High strain-rate tensile concrete behaviour, Mag. of Conc. Res. 52:365-370.

[9] Cadoni, E., Labibes, K., Albertini, C., Berra, M., Giangrasso, M. 2001. Strain-rate effect on concrete with different level of the relative humidity, *Mat. and Struct*., **34:**21-26.

[10] Comité Euro-International du Béton. Concrete structures under impact and impulsive loading. *CEB Bulletin 187*, Lausanne 1988

[11] Malvar, L.J., Ross, C.A., 1998. Review of strain rate effects for concrete in tension. *ACI Mat. J*. **95**:735–739.

[12] Rossi, P., 1991. Influence of cracking in the presence of free water on mechanical behaviour of concrete, *Mag. Conc. Res.*, **43:**53-57.

[13] Cadoni, E., Labibes, K., Berra, M., Giangrasso, M., Albertini, C. 2001. Influence of the aggregate size on the strain-rate tensile behaviour of concrete, *ACI Mat. J.*, **98**:220-223.

[14] Cadoni, E., Solomos, G., and Albertini, C., 2012. Concrete behaviour in direct tension test at high strain-rate, submitted to *Mag. of Conc. Res*.

[15] Brara, A., Klepaczko, J. R., 2007. Fracture energy of concrete at high loading rates in tension, *Int. J. of Imp. Engg.***34**:424–435.

[16] Weerheijm, J., and Van Doormaal, J.C.A.M., 2007. Tensile failure of concrete at high loading rates: New test data on strength and fracture energy from instrumented spalling tests, *Int.. J. of Imp. Engg.*, **34**:609–626.

[17] Schuler, H., Mayrhofer, M. & Thoma, K. 2006. Spall experiments for the measurement of the tensile strength and fracture energy of concrete at high strain rates. *Int.. J. of Imp. Engg.* **32**:1635-1650.